



**HAL**  
open science

## Optimization of audio graphs by resampling

Pierre Donat-Bouillud, Jean-Louis Giavitto, Florent Jacquemard

► **To cite this version:**

Pierre Donat-Bouillud, Jean-Louis Giavitto, Florent Jacquemard. Optimization of audio graphs by resampling. DAFx-19 - 22nd International Conference on Digital Audio Effects, Sep 2019, Birmingham, United Kingdom. hal-02284258

**HAL Id: hal-02284258**

**<https://inria.hal.science/hal-02284258>**

Submitted on 11 Sep 2019

**HAL** is a multi-disciplinary open access archive for the deposit and dissemination of scientific research documents, whether they are published or not. The documents may come from teaching and research institutions in France or abroad, or from public or private research centers.

L'archive ouverte pluridisciplinaire **HAL**, est destinée au dépôt et à la diffusion de documents scientifiques de niveau recherche, publiés ou non, émanant des établissements d'enseignement et de recherche français ou étrangers, des laboratoires publics ou privés.

## OPTIMIZATION OF AUDIO GRAPHS BY RESAMPLING

Pierre Donat-Bouillud

Music Representation Team  
STMS/Ircam/Inria/Sorbonne universite  
Paris, France  
pierre.donat-bouillud@ircam.fr

Jean-Louis Giavitto

Music Representation Team  
STMS/Ircam  
Paris, france  
giavitto@ircam.fr

Florent Jacquemard

Inria  
Paris, France  
florent.jacquemard@inria.fr

### ABSTRACT

Interactive music systems are dynamic real-time systems which combine control and signal processing based on an audio graph. They are often used on platforms where there are no reliable and precise real-time guarantees. Here, we present a method of optimizing audio graphs and finding a compromise between audio quality and gain in execution time by downsampling parts of the graph. We present models of quality and execution time and we evaluate the models and our optimization algorithm experimentally.

### 1. INTRODUCTION

Interactive music systems (IMS) [1] are programmable systems that combine audio signal processing with control in real-time. At run time, during a concert, they process or synthesize audio signals in real-time, using various audio effects. For that purpose, they periodically fill audio buffers and send them to the soundcard. They also make it possible to control the sound processing tasks, with aperiodic control (such as changes in a graphical interface) or periodic control (for instance, with a low frequency oscillator). Audio signals and controls are dealt with by an *audio graph* whose nodes represent audio processing tasks (filters, oscillators, synthesizers...) and edges represent dependencies between these audio processing tasks.

Puredata [2] and Max/MSP [3] are examples of IMSs. They graphically display the audio graph, but modifying it at run time as a result of a computation can be complicated. Other IMSs, such as Chuck [4] or SuperCollider [5] are textual programming languages. They are also more dynamic. In Antescofo [6], human musicians and a computer can interact on stage during a concert, using sophisticated synchronization strategies specified in an augmented score, programmed with a dedicated language, that can also specify dynamic audio graphs [7].

*Real-time constraints for audio:* Audio samples must be written into the input buffer of the soundcard periodically. The buffer size can range from 32 samples for dedicated audio workstations to 2048 samples for some smartphones running Android, depending on the target latency and the resources of the host system. For a samplerate of 44.1kHz, such as in a CD, and a buffer size of 64 samples, the audio period is 1.45 ms. It means that the audio processing tasks in the audio graph are not activated for each sample but for a buffer of samples.

IMSs are not safety critical systems: a failure during a performance is not life-critical, it will not generally result in damages or injuries. However, audio real-time processing has strong real-time constraints. Missing the deadline for an audio task, *i.e.* the time allotted by the audio driver to fill its buffer, is immediately audible:

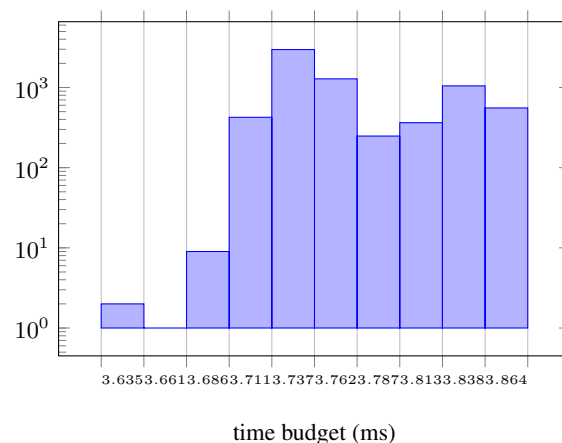


Figure 1: Histogram of relative deadlines for the *audio callback* on a MacBookPro with macOS. We execute a C++ test program generating a sawtooth signal for 10 s. The time budgets range from 3.64 ms to 3.89 ms, *i.e.* a 254  $\mu$ s jitter, with a mean of 3.78 ms

injuries. However, audio real-time processing has strong real-time constraints. Missing the deadline for an audio task, *i.e.* the time allotted by the audio driver to fill its buffer, is immediately audible:

**Buffer underflow** The audio driver uses a circular buffer the size of which is a multiple of the size of the soundcard buffer. If the task misses a deadline, it does not fill the buffer quickly enough. Depending on the implementation, previous buffers will be replayed (*gun machine* effect) or silence will be played, which entails cracks or clicks due to discontinuities in the signal. A larger buffer decreases deadline misses but increases latency.

**Buffer overflow** In some implementations, filling the buffer too quickly can also lead to discontinuities in the audio signal, if audio samples cannot be stored to be consumed later.

On the contrary, in video processing, missing a frame among 24 images per second<sup>1</sup> does not entail a visible decrease in quality so that lots of streaming protocols [8] accept to drop a frame. Therefore, real-time audio constraints are more stringent than for video. Yet, they have not been investigated as much as real-time video processing.

Composers and musicians use IMS on mainstream operating systems such as Windows, macOS or Linux, where a reliable and tight estimation of the worst case execution time (WCET) is difficult to obtain, because of the complex hierarchy of caches of the

<sup>1</sup>Although missing a key frame in a compressed stream can be visible.

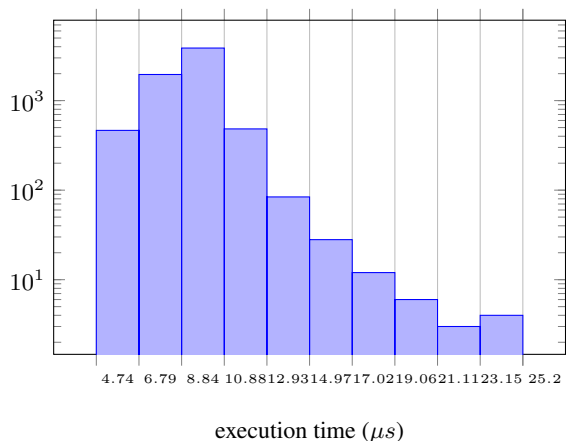


Figure 2: Histogram of the execution time for the same code generating a saw signal for 10s. Here, we show the execution time at each cycle in the *audio callback* for generating a sawtooth signal on a MacBookPro with macOS. The execution times range from 4.74 μs to 25.20 μs with an average of 9.17 μs. The standard deviation is 1.59 μs.

processor, because there are usually no real-time scheduler or temporal isolation among tasks, and because it is difficult to predict which tasks will be executed at a given time. Mainstream operating systems<sup>2</sup> are not real-time systems and do not offer any strong guarantees on deadlines for audio processing (see Fig. 1) or on the execution times (see Fig. 2). Applications that perform audio computations have to compete for CPU and memory resources with other applications during a typical execution. Those platforms are also often on batteries and often change the frequency of the CPUs in order to save energy, thus totally changing execution times. It follows that we cannot assume that we know the WCET of tasks. Furthermore, IMSs are more and more ported to embedded cards such as Raspberry Pi and have to adapt to limited computation resources on these platforms. On the other hand, composers and sound designers create more and more complex musical pieces, with lots of dynamically interconnected nodes, using a sampling rate up to 96 kHz.

Hard real-time scheduling algorithms that depend on knowing the WCET cannot be applied here, as in practice, IMSs are executed on those operating systems without strong real-time guarantees.

When real-time constraints are not critical, modifying the quality of service (QoS) by partially executing some tasks or even discarding them is an option to consider. In the case of IMSs, tasks are dependent, with dependencies defined with the edges of the audio graph. The quality of a task is itself *position-dependent*: it depends on the position of the audio processing task in a path going from an audio input to an audio output. It means we cannot merely discard or degrade any task in the audio graph, to achieve an optimal QoS adaptation.

To deal with these challenges, IMSs have rather chosen to increase the available computation resources, in particular by increasing the parallelism of the audio graphs in scores to take advantage of the multicore processors. For example, an alterna-

<sup>2</sup>There is an earliest deadline first scheduler [9] on Linux, but it's typically not activated on mainstream distributions.

tive scheduler for SuperCollider, Supernova [10], can use several cores to synthesize sounds. However, these new schedulers do not automatically parallelize the audio graph but require explicit instructions, such as `ParGroup` for SuperCollider, or `poly` for Max/MSP, and so are difficult to program.

In this paper, we propose an alternative solution where we explore how an audio graph can be optimized by degrading audio processing units without perceiving the degradations (or minimizing the degradation perception). The idea is to generate an *equivalent* but degraded audio graph where the execution time of the graph is decreased while decreasing the quality of the audio processing tasks.

Because of the dependencies, we do not degrade only a single task here, but we have to *choose a whole set of dependent nodes* in an audio graph to degrade. We aim at finding paths to degrade in the audio graph, where the quality of a task is position-dependent. The nodes are seen as *blackboxes* and degradations are made by *resampling* the signal flowing between nodes.

We describe a model of an audio graph based on the dataflow paradigm [11] with models of execution time and quality. We present an *offline* algorithm based on the models that explores exhaustively or randomly the possible degraded versions of an audio graph with constraints on execution time and quality. Heuristics help to select subpaths to degrade in the audio graph at execution time. We evaluate our optimization strategy on three different sets of audio graphs : an exhaustive enumeration of all possible graphs with few nodes, a random sampling of graph with many nodes, and graphs structurally generated from Puredata patches.

## 2. RELATED WORK

Degrading computations to achieve to respect some time criterion has been dealt with in the *approximate programming* paradigm or in real-time system theory, with *mixed criticality*.

Approximate computing [12] is a paradigm in which errors are allowed in exchange of an improvement of performance. The concept of correctness is relaxed to a correctness with a quantitative error. In [13], a graph is used to represent a *map-reduce* program, with map nodes which compute and reduce nodes which aggregate data. Offline, they generate approximate versions of the graph with a given precision. For that purpose, two kinds of transformations are considered: *substitution transformations* and *sampling transformations*, where the input is randomly downsampled. However, this model is aimed at batch-processing, not real-time audio graphs.

In multimedia systems, a basic strategy [14] related to mixed criticality consists of dividing tasks between a mandatory and an optional part, which can be discarded in case of overload of the processor. Real-time scheduling with this strategy does not entail too much overhead but does not handle dependencies between tasks, in particular for quality estimation. Some mixed criticality approaches address graph-based tasks for mixed-criticality systems, such as in [15]. However, the dependencies between tasks are functional dependencies: all tasks in a graph have the same criticality but it is possible to switch to other graphs with another criticality. Criticality levels are not like *qualities* that would depend on the topology of the graph.

### 3. MODEL OF AN AUDIO GRAPH

#### 3.1. Model of an audio graph

In an audio graph, audio streams flow between signal processing nodes at various rates, depending on what the nodes require. The *dataflow* model [11, 16] is well suited to describe these kinds of dependent tasks. In the usual *dataflow* model, no time information is provided, so we enrich this *dynamic dataflow* model with temporal information, such as start times or average execution times (ACET), as in the Time-Triggered Dataflow mode [17]. We also define a quality measure on the graph.

#### 3.2. Dataflow model

The *dataflow* model is *data-oriented*: when there are enough data, seen as a sequence of *tokens*, on a node, the node is fired, consequently, yielding some tokens. More formally, we use the port graph formalism, as in [18]. A *dataflow* quadruplet  $G = (V, P, E, \mu)$  where the vertices in  $V$ , represent the signal processing nodes and are pairs  $(I, O)$  with  $I \subset P$  and  $O \subset P$ , the input and output ports. The edges in  $E \subset P \times P$  represent the data flowing between vertices and connect an *output* ports of a vertice to an *input* port of another vertice. We note  $p_1 \rightarrow p_2$  the edge between ports  $p_1$  and  $p_2$ ;  $v_1 \rightarrow v_2$  would denote any edge  $v_1.p \rightarrow v_2.p'$  between  $v_1$  and  $v_2$ . We note  $v.p$  the port  $p$  of vertice  $v$ . The function  $\mu : P \rightarrow \mathbb{N}$  maps a port to the number of audio samples it consumes or produces.

**Distinguished nodes** The nodes without input ports are called *inputs* or *sources*. They are typically audio stream generators. The nodes without output ports are the *outputs* or *sinks*, as shown in Fig. 3. They are audio sinks to the soundcard for instance. Nodes that are neither *inputs* nor *outputs* are called *effects*.

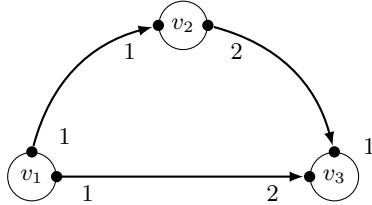


Figure 3: A simple *synchronous dataflow* graph with three nodes  $v_1, v_2$  and  $v_3$  with only one input port and one output port for each of them. Data flows from  $v_1$  to  $v_3$ , from  $v_1$  to  $v_2$  and from  $v_2$  to  $v_3$ .  $v_1$  yields 1 token per firing, and  $v_3$  requires 2 tokens to be fired.  $v_1$  is a *source* node,  $v_3$  a *sink* node.

#### 3.3. Timed dataflow

A *dataflow* graph only describes the partial ordering of the firing of its nodes, but not their firing time instants. However, *dataflow* graphs are often used to describe real-time processing, including audio signal real-time processing. In the following, *input* nodes are given firing dates and *output* nodes, deadlines. Any node  $v$  gets an average case execution time (ACET),  $A_v$  and a worst case execution time (WCET),  $W_v$ . Although we will evaluate the model with the ACET, we could also evaluate with the WCET if we had an accurate WCET. We will note  $T_v$  the execution time of a node. We also assume that the graph is acyclic.

The audio processing nodes are periodic and we note  $s_v^1 \dots s_v^n$  with  $s_v^i < s_v^{i+1}$  the firing times of node  $v$ , where  $s_v^{i+1} - s_v^i = s_v^2 - s_v^1 = T_v$  with  $T_v$  the period of node  $v$ . The samplerate  $f_{p_v}$  on a port  $p_v$  of node  $v$  is  $\frac{\mu(p_v)}{T_v}$ .

**Execution time of a path** On a path  $\pi = v_1 \rightarrow \dots \rightarrow v_n$ , the mean execution time (resp. worst case) is  $\sum_{i=1}^n A_{v_i}$  (resp.  $\sum_{i=1}^n W_{v_i}$ ).

**Execution time of the whole graph** For the whole graph  $G$ , on a parallel system with enough resources, the execution time is the largest execution time of a path between inputs and outputs, *i.e.* for the ACET,  $A_G = \max_{\pi \in \text{Path}} \{A_\pi\}$ . For instance, for Fig. 3:

$$A_G = \max\{A_{v_1 \rightarrow v_3}, A_{v_1 \rightarrow v_2 \rightarrow v_3}\}$$

In a sequential execution mode (for instance on a uniprocessor), it is the sum of the execution times of all the nodes:

$$A_G = \sum_{v \in G} A_v \quad (1)$$

**Estimating  $A_v$**  We measure the average execution time  $A_v$  of all the possible nodes that can be part of the audio graph. We do not care about the exact execution time, but rather of an ordering on the execution times between various versions of an audio graph. In addition, the execution time increases monotonically with the buffer input sizes. Thus, we only measure the average execution of a given buffer size. However, some nodes can have a variable number of inputs and outputs, such as a `MIXER` node. We do not want to measure all possible combinations of inputs and outputs. Experimentally, we find that the average case execution time  $A_{\text{mixer}}(n_{\text{inputs}}, n_{\text{outputs}})$  of a mixer with  $n_{\text{inputs}}$  and  $n_{\text{outputs}}$  is given by:

$$\begin{aligned} A_{\text{mixer}}(n_{\text{inputs}}, n_{\text{outputs}}) &= n_{\text{inputs}} \times \underbrace{(A_{\text{mixer}}(2, 1) - A_{\text{mixer}}(1, 1))}_{\text{cost of adding}} \\ &+ n_{\text{outputs}} \times \underbrace{(A_{\text{mixer}}(1, 2) - A_{\text{mixer}}(1, 1))}_{\text{cost of copying one buffer}} \end{aligned} \quad (2)$$

#### 3.4. Quality

The quality of the audio graph is a subjective matter, and relates to psychoacoustics. It depends on the semantics of the nodes. We aim at designing an *a priori* quality measure based on parameters of the audio effects, which is more practical to compute in real-time than analysing the audio signal.

The quality measure should be *compositional*, *i.e.* the quality of the graph  $q_G \in [0, 1]$  must be a function of the quality of its nodes and edges. The worst quality is 0 and the best quality is 1. For each node  $v$ , we also note  $q_v \in [0, 1]$  its quality.

We define the quality  $q_{v_1 \rightarrow \dots \rightarrow v_n}$  on a path  $v_1 \rightarrow \dots \rightarrow v_n$  as  $q_{v_1} \otimes \dots \otimes q_{v_n}$  for an operator  $\otimes$  with the following properties:

**Associativity**  $q_{v_1} \otimes (q_{v_2} \otimes q_{v_3}) = (q_{v_1} \otimes q_{v_2}) \otimes q_{v_3}$

**Decreasing**  $q_v \otimes q_{v'} \leq q_{v'}$ . It means that quality never increases on the path, as the information lost by degrading cannot be rebuilt.

**Identity element** There is an identity element  $1_\otimes$  such that  $1_\otimes \otimes v = v \otimes 1_\otimes = v$ . Such an element is the quality which preserves for the output the quality of its input.

An obvious choice for an operator fulfilling these desired properties is multiplication on real numbers. For  $v \rightarrow v'$ :

$$q_{v \rightarrow v'} = q_v \otimes q_{v'} = q_v \times q_{v'}$$

On the path  $v_1 \rightarrow \dots \rightarrow v_n$ , thanks to associativity:

$$q_{v_1 \rightarrow \dots \rightarrow v_n} = \prod_{i=1}^n q_{v_i} \quad (3)$$

We also define a *join* operator  $\oplus$  that models the quality resulting from joining two paths, such as  $v_1 \rightarrow v_3$  and  $v_1 \rightarrow v_2 \rightarrow v_3$  on Fig. 3.

$$\begin{aligned} q_G &= q_{v_1 \rightarrow v_3} \oplus q_{v_1 \rightarrow v_2 \rightarrow v_3} \\ &= (q_{v_1} \otimes q_{v_3}) \oplus (q_{v_1} \otimes q_{v_2} \otimes q_{v_3}) \end{aligned} \quad (4)$$

In practice, we choose  $\bigoplus_{k=1}^n q_k = \frac{1}{n} \sum_{k=1}^n q_k$  for  $n$  joining paths for mixer-like nodes and  $\oplus = \min$  for the other nodes.

#### 4. OPTIMIZATION BY RESAMPLING

We consider a method of degrading the quality which is agnostic of the actual computation node semantics, as it operates on the signal that flows in-between the nodes by resampling parts of the audio graph. The rationale for resampling is based on the following cognitive observations. Above some frequency threshold, no quality improvement is perceived by human beings, according to psychoacoustics studies [19]. Indeed, the human auditory system cannot perceive frequency above 20 kHz. Shannon's theorem implies that the sampling rate must be at least double of the maximum frequency, so about the sampling rate of audio CDs of 44.10 kHz. However, oversampling makes it possible to better handle rounding errors in the signal processing and that is why we also consider frequencies higher than 44.10 kHz.

##### 4.1. Resampling a signal path

###### 4.1.1. Inserting resampling nodes

In a dataflow graph, nodes are fed with samples. The premise here is that a node which receives less samples will take less time to be executed. Changing the number of samples per time unit is a common operation in signal processing, called *resampling*: getting less is *downsampling*, and more, *upsampling*. In order to resample, we insert resampling nodes in the graph. These nodes have the same attributes and properties as other nodes: they can interpolate between samples, copy samples in audio buffers. They have a quality measure and temporal characteristics such as a ACET or WCET, so that we can take into account the overhead due to inserting those nodes. Every resampling node has one input port and one output port.

When a downsampling node is inserted on a path, all the following nodes in the path operate on a downsampled signal. We need to insert an upsampling node if there is a node on that path that enforces a specific samplerate, typically, a sink to the sound-card.

We consider a path  $\pi = v_1 \rightarrow \dots \rightarrow v_n$  where for a node  $v_k$  in path  $\pi$ ,  $v_k = (\{p_{k,j}^i\}, \{p_{k,j}^o\})$  with  $p_j^{ki}$  the input ports and  $p_j^{ko}$  the output ports. Thus, the degraded path  $\pi'$  is  $\pi' = v_1 \rightarrow v'_1 \rightarrow \dots \rightarrow v'_n \rightarrow v_n$ . We want to insert downsampling node  $v'_1$  just after  $v_1$  and an upsampling node  $v'_n$  just before  $v_n$ , as shown

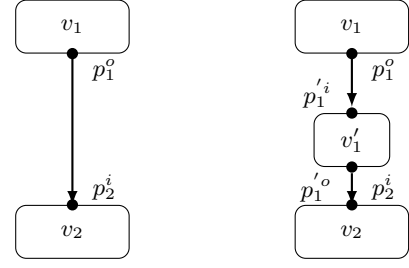


Figure 4: Inserting a downsampling node  $v'_1$  between nodes  $v_1$  and  $v_2$ .  $v_1$  has an output port  $p_1^o$ ,  $v_2$  has an input port  $p_2^i$  and  $v'_1$  has an input port  $p_1'^i$  and an output port  $p_1'^o$ .

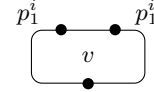


Figure 5: Node  $v$  is on path  $v_1 \rightarrow \dots \rightarrow v_n$ . The resampled signal flows on this path through input port  $p_1^i$  with resampling factor  $q$ . Node  $v$  has another input port,  $p_2^i$ . The signal coming into this port must also be resampled with resampling factor  $r$ .

in Fig. 4. The resampling factor of  $v'_1$  is  $r \in \mathbb{Q}$  such that  $\mu(p_1'^i) = \mu(p_1^o)$  and  $\mu(p_1'^o) = r \times \mu(p_1^i)$  for all edges between, *i.e.* the input of the resampling node is at the same rate at its incoming node, and its output is at the new rate. We do it in the same way when inserting an upsampler,  $r \geq 1$ , and for an upsampler,  $r \geq 1$ . For all  $k \in \llbracket 2, n-1 \rrbracket$ , the rates of all input and output ports of node  $v_k$  are multiplied by the resampling factor  $r$  of  $v'_1$ .

In case a node on the path has several input ports and that one of them receives a resampled signal, we also have to resample by the same resampling factor the other input ports, as shown in Fig. 5, by inserting a resampling node connected to this input port.

Also, if an output port  $p$  of node  $v$  is connected to several input ports  $p_1, \dots, p_n$ , it is more efficient to insert the resampler and then a node with  $n$  outputs, instead of inserting a resampler on each edge  $p \rightarrow p_k$ , as shown in Fig. 6.

###### 4.1.2. Execution times

We assume that the computation nodes process all their incoming samples and hence, that the complexity of their computations is at least linear. So we can bound execution times of  $v_k$  for  $k \in \llbracket 2, n-1 \rrbracket$  for a downsampler with resampling factor  $1/t$ :

$$A'_{v_k} \leq \frac{1}{t} \times A_{v_k} \quad (5)$$

$$W'_{v_k} \leq \frac{1}{t} \times W_{v_k} \quad (6)$$

We can deduce a bound on the whole execution times of the degraded path  $\pi'$ :

$$A'_\pi \leq A_{v_1} + A_{v'_1} + \frac{1}{t} \times \sum_{k=2}^{n-1} A_{v_k} + A_{v'_n} + A_{v_n} \quad (7)$$

that is to say for the subpath:

$$A'_\pi \leq A_{v_1} + A_{v'_1} + \frac{1}{t} A_{v_2 \rightarrow \dots \rightarrow v_n} + A_{v'_n} + A_{v_n} \quad (8)$$

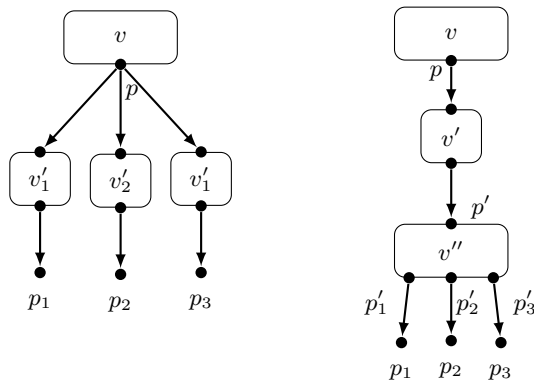


Figure 6: Node  $v$  has one output port,  $p$ , which is connected to three input ports,  $p_1, p_2, p_3$ . On the left, we insert a resampler on each edge  $p \rightarrow p_1, p \rightarrow p_2, p \rightarrow p_3$  whereas on the right, we insert a node  $v''$  with one input port  $p'$  and 3 outputs  $p'_1, p'_2, p'_3$ , and we insert the resampler  $v'$  on edge  $p \rightarrow p'$ .

Note that we take into account the execution times of the inserted nodes, so that the optimization is *overhead-aware*. For small graphs with audio processing nodes with an execution time in the same order of magnitude of the resamplers, the execution time of a degraded graph can be actually larger than the non-degraded one.

#### 4.1.3. Quality

The *a priori* quality measure in the case of resampling is the sampling rate: the lower the sampling rate, the lower the quality. In the case of path  $\pi$ , we have  $f_{v'_1} = \frac{q \times \mu(p'_1)}{T_{v'_1}}$ . If audio is sent too late to the output buffer, a click can be heard. We consider that it is worse to hear a click because of missing the deadline of the audio driver than to hear a resampled signal. A node that would entail always missing deadlines is given the worst possible quality. The quality  $q_v$  of a downsampled node is such that  $q_v < 1_{\otimes}$ . The quality of a non-downsampled node is 1.

## 4.2. Degraded versions

Choosing the nodes to degrade in the audio graph is an optimisation problem under constraints. We can try to maximize the quality of the audio graph given an execution time constraint (a deadline), or minimize the execution time of the audio graph given a minimum target quality.

Our system can enumerate all the possible degraded versions of a graph, or a random sampling of the degraded versions, or use heuristics to compute a useful subset that respects some constraints. The tool is an open source OCaml program<sup>3</sup> that accepts Puredata or MAX/MSP patches, or a custom format as input and can output one optimized version or a set of optimized versions.

#### 4.2.1. Exhaustively

Enumerating all the possible degraded versions of the audio graph is enumerating all the possible subsets of nodes that can be degraded in the audio graph, *i.e.* all nodes except sources and sinks.

<sup>3</sup><https://github.com/programLyrique/ims-analysis>

Then resamplers are inserted so that all the chosen nodes are degraded and the nodes stay isochronous, that is to say have the same sample rate for all input ports and the same sample rate for output ports.

The number of degraded versions is  $\mathcal{O}(2^n)$  where  $n$  is the number of nodes in the graph and so is impractical when audio graphs start to have a huge number of nodes. When  $n$  is large, we randomly choose the possible degraded versions and make sure we have the non-degraded graph and the fully-degraded graph<sup>4</sup> in the set.

#### 4.2.2. Heuristics

The idea is to degrade nodes starting from the outputs, as inserting a downsampling node near the end of the branch impact less nodes than at the beginning.

We choose to have at most one resampled subpath per branch. We also try to minimize the number of inserted nodes with respect to the number of degraded nodes on the resampled subpath, in order to minimize the overhead due to resampling nodes. For that, we need to minimize the number of branches where we resample and that is why we explore the graph branch per branch.

We can use this heuristics to find approximate solutions the optimization problem of maximizing the quality with an execution time constraint. For that, we start from one of the output nodes, and we traverse the graph backwards and see how inserting a downsampling node on a path going to this output node would change the estimated remaining execution time, until the estimation of remaining execution time is lower than the remaining time before the deadline. Other branches can be explored if it is not enough. Then the downsampling and upsampling nodes are inserted on the paths chosen to be resampled.

## 5. EXPERIMENTAL EVALUATION

In order to evaluate our theoretical models, we need to instantiate our models on a large number of graphs. However, there are no reference benchmarks of audio graphs for IMS. We decided to generate a huge number of graphs, compute the theoretical execution time (in Sect. 3.3) and quality (in Sect. 3.4) of each graph, and then measure the execution time and a quality based on the actual audio signal. We then compare the theoretical values and the measured ones.

The resamplers in use for these experiments are the linear resamplers, and we only resample by 2.

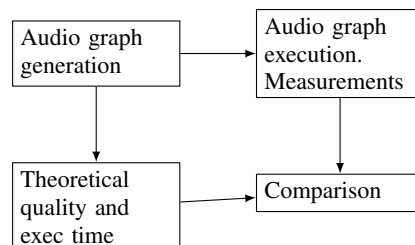


Figure 7: The experimental setup to evaluate the models of quality and execution time.

<sup>4</sup>The audio graph where all the inner nodes are downsampled. It has the worst possible quality and possibly the shortest execution time.

## 5.1. Measuring execution time and quality

We developed a open source rust program<sup>5</sup> that can execute the audio graph, monitor execution times of the audio callback, and output the resulting audio. The resampling is handled by `libsamplerate`,<sup>6</sup>. This is an *opensource* library that makes it possible to downsample down to a 256 ratio, and to upsample up to a 256 ratio. The sampling rate can be changed in real-time. The library provides five resamplers, classified by decreasing order of quality: best, medium, faster sync resamplers (as in [20]), zero order hold resampler, and a linear resampler.

**Measuring execution time** We execute the audio graph for a large number of cycles and drop the first cycles to take into account processor cache warming.

**Measuring quality** We compare the audio signal of a degraded graph and the one of the non-degraded graph. Given the spectrum of each signal, we compute their constant-Q transform [21], as we are interested in music signals. We then use a psychoacoustics curve called A-weighting [22] to account for the limited hearing range of human beings (up to 20 kHz). Finally, we compute the distance between the two resulting spectra and normalize it so that a distance of 0 is a quality of 1 and, of  $+\infty$ , a quality of 0:

$$q_G^{\text{mes}} = \exp(-\|s_{\text{non\_degraded}} - s_G\|) \quad (9)$$

## 5.2. Comparing the model and the measurements

### 5.2.1. Graph generation

We generate the structure of the graphs first, *i.e.* vertices and edges, and then pick actual audio processors for each vertex in a node dictionary.

**Exhaustive generation for a given number of nodes** We enumerate all the non-labelled WCDAGs with  $n$  vertices. Non-labelled entails that  $a \rightarrow b$  and  $b \rightarrow a$  are isomorphic, are the *same* graphs. Given the set of vertices  $V = \{0, \dots, n-1\}$ , we undertake the following steps:

1. Compute the set of all the possible edges  $\mathcal{E}$  between distinct vertices in one direction. For that, we remark that  $\text{pairs}(a_k, \dots, a_n) = \bigcup_{i \in \{k+1, \dots, n\}} \{(a_k, a_i)\} \cup \text{pairs}(a_{k+1}, \dots, a_n)$  It will entail acyclicity.
2. Compute  $\mathcal{P}(\mathcal{E})$
3. In a connected graph with  $n$  vertices, there are at least  $n-1$  edges (*i.e.* a chain graph). So we keep only subsets with more than  $n$  edges of  $\mathcal{P}(\mathcal{E})$  in our admissible set of set of edges,  $E$ .
4. Build the set  $D$  of DAGs from  $E$ , one graph per subsets.
5. Filter  $D$  to remove non weakly-connected graphs, by picking a node and then traverse the undirected version of the graph and counting the vertices. If there are the same numbers as the total number of vertices in the graph, it is weakly connected.

The set of all possible edges from  $n$  nodes has size:

$$(n-1) + n-2 + \dots + 1 = \sum_{k=1}^{n-1} k = \mathcal{O}(n^2) \quad (10)$$

<sup>5</sup><https://github.com/programLyrique/audio-adaptive-scheduling>

<sup>6</sup><http://www.mega-nerd.com/SRC/>

Thus the powerset has size  $\mathcal{O}(2^{n^2})$ . The following operations reduce the number of graphs so we keep that upper bound.

**Random generation** As the increase in the number of graphs is over-exponential, it becomes untractable when  $n > 6$  in practice. For  $n = 7$  for instance, there are 3781503 possible DAGs. Hence, for larger number of nodes, we randomly generate graphs using the Erdős–Rényi [23] random graph mode, where a graph can be chosen uniformly at random from the graphs with  $n$  nodes and  $M$  edges, or with  $n$  nodes and a given probability of having an edge between two edges.

**From Puredata patches** Audio graphs tend to exhibit a particular structure: few incoming and outgoing edges per node, creating long chains in the audio graph, with a few nodes with more inputs that typically mix signals. To take into account this structure, we parsed all the Puredata patches of its tutorial and examples (*i.e.* 133 graphs).

**Picking the actual nodes** We maintain a database of possible audio processing nodes, with their estimated execution time, their numbers of input ports and output ports, and their possible control parameters. The possible parameter values can be annotated with a range,  $[0, 1]$  for instance for a volume, or a set, for instance  $\{20, 440, 1000, 2500, 6000\}$  for a set of frequencies.

Given the structure of the graph, for each vertex in it, we can pick (or generate all possible versions) of nodes with the same number input ports as of incoming edges and a number of output ports between 1 and the number of outgoing edges. For the output ports, it is due to *port sharing*, as shown in Fig. 8.

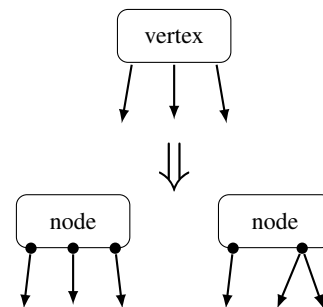


Figure 8: Port sharing entails that a vertex can be replaced by a node with not the same number of output ports, due to port sharing. At the top, it is a vertex with 3 outgoing edges. At the bottom, we show two possible actual nodes from this vertex, one with 3 output ports, and one with 2 output ports and the second port shared by two outgoing edges.

### 5.2.2. Comparing rankings

After generating the graphs, we can both compute the theoretical qualities and execution times, and measure the actual ones. We obtain two permutations of our set of graphs and we need to know how far the two permutations are.

To compare the similarity of the orderings of the graphs ranked by the theoretical and measured quantities, we use *rank correlation*. The Kendall rank correlation coefficient (Kendall’s tau coefficient) [24] is linked to the number of inversions needed to transform one ordering into the other one. The Spearman’s rank correlation coefficient (or Spearman’s rho) [25] is linked to the distance

in positions of a same graph in the two orderings. If the correlation is +1, the two orderings are ranked in the same way, *i.e.* the function that transforms one into the other one is monotonic. If it is -1, the order is reversed.

We also compare the position in the two orderings of the worst quality graphs, the shortest execution time and the longest execution time.

### 5.2.3. Results

**Exhaustive enumeration** For Fig. 9, we enumerated all the audio graphs with 5 nodes, that is to say, 838 graphs. The average number of versions of a non degraded graph (including the non-degraded graph) is  $3.657518 \pm 2.066605$  and there are 57 graphs without degraded versions. The theoretical models and the measurements both of execution time and quality are well correlated. There are so many correlations in the 0.9 – 1 bin because many 5 nodes graphs have few degraded versions.

Only 22, *i.e.* 2%, degraded graphs are quicker to execute than their degraded versions here when using nodes with execution time the same order of magnitude as the resamplers. Indeed, in that case, the length of a resampled branch must be large for it to execute quicker than the non-degraded version. However, small graphs do not exhibit long branches. On the contrary, when using nodes an order of magnitude bigger, 275, *i.e.* 33% degraded graphs are quicker than their non-degraded version.

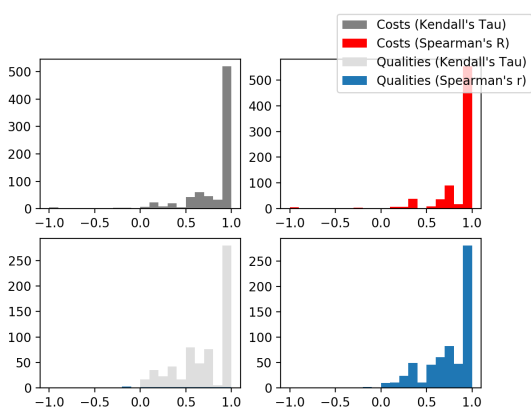


Figure 9: Correlations for an exhaustive enumeration of 5-node audio graphs. At the top, execution times (costs), at the bottom, qualities; on the left, Kendall's Tau, on the right, Spearman's R.

**Large random graphs** For Fig. 10, we generated 100 random graphs with 10 nodes and a 0.3 edge probability, in order to have nodes with not too many inputs and outputs, as in real audio graphs. The execution time model is rather accurate, with most correlations above 0.5. For the quality, the results are less good, as there are lots of correlations close to 0, but mainly strictly positive. With quick nodes, 15 graphs have degraded versions quicker than their non-degraded versions, whereas with slow nodes, there are 45.

**With graphs from Puredata** For Fig. 11, we generated 133 audio graphs from 133 Puredata patches. The model of execution time is accurate, which is especially visible with the Spearman correlation coefficient histogram. The model of quality and the measurement of qualities are better correlated than for random

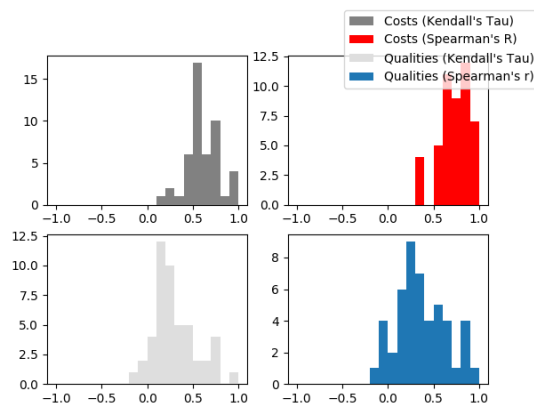


Figure 10: Correlations for random 10-node audio graphs with 0.3 edge probability. At the top, execution times, at the bottom, qualities; on the left, Kendall's Tau, on the right, Spearman's R.

graphs. With quick nodes, 48 graphs, *i.e.* 36%, have degraded versions which are quicker than the non-degraded graph. The structure of Puredata graphs exhibit longer branches and more subsets of the graph that can be resampled with just a few resamplers.

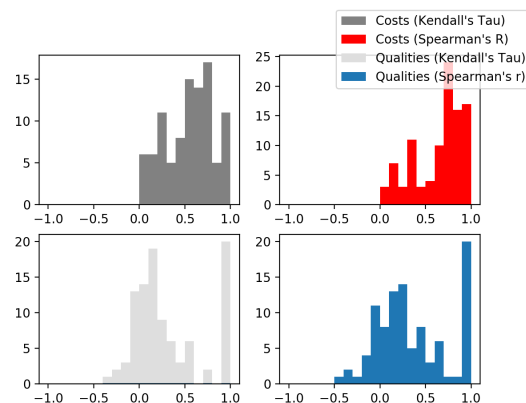


Figure 11: Correlations for audio graphs generated from Puredata patches. Node count can go up to 80. At the top, execution times, at the bottom, qualities; on the left, Kendall's Tau, on the right, Spearman's R.

Hence, large graphs without too many ramifications, and with nodes with execution times at least an order of magnitude higher than the execution time of a resampler take advantage the most of the resampling optimization. Actual audiographs from IMSs, such as the ones from Puredata, have actually these characteristics.

## 6. CONCLUSION

We proposed a model of an audio graph with execution time and quality, and an optimization algorithm based on the models that can find degraded versions of an audio graph while respecting constraints on execution time or quality. The degradations are based on downsampling parts of the graph.



We evaluated the models and the algorithm on audio graphs that were exhaustively enumerated for graph with few nodes, randomly generated for larger graphs, and generated from Puredata patches. The execution time model is quite accurate. The quality model is well correlated for small graphs (Fig. 9), has to be improved on large random graphs (Fig. 10) and promising results are obtained for graphs (Fig. 11) generated from real Puredata patches. The optimization is particularly effective for actual audio graphs with long audio effects and long branches. Our choice of measures of quality is arbitrary. Another option would be to organize listening tests, but would be impractical considering the huge size of the set of possible graphs and possible degraded graphs.

The optimization program can be integrated to the design of an audio graph, using our custom audio graph format that describes nodes and their connections as input and output and can import Puredata patches but we aim at making it easier to use within MAX/MSP and Puredata. We also want to integrate our optimization as a compiler optimization for Faust programs in the Faust compiler [26]. It would unlock access to many more different audio graphs. As the Faust instructions are both very fine-grained and well-defined, we would be able to refine the execution time and the quality models.

## 7. ACKNOWLEDGMENTS

This work started during a visit in the group of Prof. Christoph Kirsch in Salzburg, whom we would like to thank for his advice. We also would like to thank the anonymous reviewers for their insights and advice.

## 8. REFERENCES

- [1] Robert Rowe, *Interactive Music Systems: Machine Listening and Composing*, AAAI Press, 1993.
- [2] M. Puckette, “Using pd as a score language,” in *Proc. Int. Computer Music Conf.*, September 2002, pp. 184–187.
- [3] David Zicarelli, “How I learned to love a program that does nothing,” *Comput. Music J.*, vol. 26, no. 4, pp. 44–51, 2002.
- [4] G. Wang, *The ChucK audio programming language. A strongly-timed and on-the-fly environ/mentality*, Ph.D. thesis, Princeton University, 2009.
- [5] James McCartney, “Supercollider: a new real time synthesis language,” in *Proceedings of the International Computer Music Conference*, 1996.
- [6] José Echeveste, Arshia Cont, Jean-Louis Giavitto, and Florent Jacquemard, “Operational semantics of a domain specific language for real time musician–computer interaction,” *Discrete Event Dynamic Systems*, vol. 23, no. 4, pp. 343–383, 2013.
- [7] Pierre Donat-Bouillud, Jean-Louis Giavitto, Arshia Cont, Nicolas Schmidt, and Yann Orlarey, “Embedding native audio-processing in a score following system with quasi sample accuracy,” in *ICMC 2016-42th International Computer Music Conference*, 2016.
- [8] Saamer Akhshabi, Ali C Begen, and Constantine Dovrolis, “An experimental evaluation of rate-adaptation algorithms in adaptive streaming over http,” in *Proceedings of the second annual ACM conference on Multimedia systems*. ACM, 2011, pp. 157–168.
- [9] Dario Faggioli, Fabio Checconi, Michael Trimarchi, and Claudio Scordino, “An edf scheduling class for the linux kernel,” in *Proceedings of the Eleventh Real-Time Linux Workshop*. Citeseer, 2009.
- [10] T. Blechmann, “Supernova—a multiprocessor aware real-time audio synthesis engine for supercollider,” M.S. thesis, Vienna University of Technology, 2011.
- [11] Edward A Lee and David G Messerschmitt, “Synchronous data flow,” *Proceedings of the IEEE*, vol. 75, no. 9, pp. 1235–1245, 1987.
- [12] Swagath Venkataramani, Srimat T Chakradhar, Kaushik Roy, and Anand Raghunathan, “Computing approximately, and efficiently,” in *Proceedings of the 2015 Design, Automation & Test in Europe Conference & Exhibition*. EDA Consortium, 2015, pp. 748–751.
- [13] Zeyuan Allen Zhu, Sasa Misailovic, Jonathan A Kelner, and Martin Rinard, “Randomized accuracy-aware program transformations for efficient approximate computations,” in *ACM SIGPLAN Notices*. ACM, 2012, vol. 47, pp. 441–454.
- [14] Jane WS Liu, Kwei-Jay Lin, Wei Kuan Shih, Albert Chuang-shi Yu, Jen-Yao Chung, and Wei Zhao, *Algorithms for scheduling imprecise computations*, Springer, 1991.
- [15] Pontus Ekberg and Wang Yi, “Schedulability analysis of a graph-based task model for mixed-criticality systems,” *Real-time systems*, vol. 52, no. 1, pp. 1–37, 2016.
- [16] Edward A Lee and Thomas M Parks, “Dataflow process networks,” *Proceedings of the IEEE*, vol. 83, no. 5, pp. 773–801, 1995.
- [17] Pau Arumí and Xavier Amatriain, “Time-triggered static schedulable dataflows for multimedia systems,” in *Multimedia Computing and Networking 2009*. International Society for Optics and Photonics, 2009, vol. 7253, p. 72530D.
- [18] Oana Andrei and H elene Kirchner, “A rewriting calculus for multigraphs with ports,” *Electronic Notes in Theoretical Computer Science*, vol. 219, pp. 67–82, 2008.
- [19] Stuart Rosen and Peter Howell, *Signals and systems for speech and hearing*, vol. 29, Brill, 2011.
- [20] Julius O Smith and Phil Gossett, “A flexible sampling-rate conversion method,” in *Acoustics, Speech, and Signal Processing, IEEE International Conference on ICASSP’84*. IEEE, 1984, vol. 9, pp. 112–115.
- [21] Judith C Brown, “Calculation of a constant q spectral transform,” *The Journal of the Acoustical Society of America*, vol. 89, no. 1, pp. 425–434, 1991.
- [22] Brian CJ Moore, *An introduction to the psychology of hearing*, Brill, 2012.
- [23] Paul Erdős and Alfr ed R enyi, “On the evolution of random graphs,” *Publ. Math. Inst. Hung. Acad. Sci.*, vol. 5, no. 1, pp. 17–60, 1960.
- [24] Maurice George Kendall, “Rank correlation methods,” 1948.
- [25] Wayne W Daniel et al., *Applied nonparametric statistics*, Houghton Mifflin, 1978.
- [26] Yann Orlarey, Dominique Fober, and Stephane Letz, “Syntactical and semantical aspects of faust,” *Soft Computing*, vol. 8, no. 9, pp. 623–632, 2004.